UNCERTAINTY PROPAGATION FOR SELECTED ANALYTICAL MILLING STABILITY LIMIT ANALYSES

G. Scott Duncan, Mohammad H. Kurdi, Tony L. Schmitz
Department of Mechanical and Aerospace Engineering
University of Florida
Gainesville, FL

John P. Snyder
TechSolve
Cincinnati, OH

KEYWORDS

Machining, stability, chatter, lobe, accuracy.

ABSTRACT

This paper describes the propagation of uncertainty contributors through the analytical milling stability models developed by Tlusty *et al*. and Altintas and Budak. These analyses provide graphical representations of the limiting axial depth of cut for chatter-free milling as a function of spindle speed in the form of stability lobes. In this work, confidence intervals are added to these stability lobes to improve their utility at the shop floor level. Using Monte Carlo simulation techniques, uncertainties in the model inputs, including the tool point frequency response function, cutting force model coefficients, and radial depth of cut, are used to determine the associated uncertainty in the predicted stability limit at each spindle speed.

INTRODUCTION

As stated in NIST Technical Note 1297 [Taylor and Kuyatt], 'the result of a measurement is only an approximation or estimate of the value of the specific quantify in question, that is, the measurand, and thus the result is complete only when accompanied by a quantitative statement of its uncertainty'. The inclusion of a defensible uncertainty statement enables the user to determine his/her confidence in the measurement and its usefulness in decision making. This concept can be extended to simulation results based on measured input quantities. Again, the user requires some indication of the reliability of the analysis output to gage its usefulness.

Guidelines for evaluating the uncertainty in measurement results are described in [ISO, ANSI, Taylor and Kuyatt, and Bevington and Robinson], for example. Often the measurand is not observed directly, but is expressed as a mathematical function of multiple input quantities. In this case, the fundamental steps in uncertainty estimation are to define the measurand, identify the input uncertainty contributors and their distributions, and propagate the uncertainties through the measurand using either analytical (Taylor series expansion) or sampling (Monte Carlo, Latin hypercube) approaches.

The goal of this work is to identify the combined standard uncertainty, u_c, which

incorporates the separate influences of the variances in the input uncertainties and represents one standard deviation of output variation, of the milling stability limit as defined by the analytical analyses of [Tlusty *et al*.] and [Altintas and Budak]. Because the stability limit is described as a function of spindle speed, u_c is also a function of spindle speed in this analysis. In this treatment, potential limitations of the stability models will not be considered as part of the uncertainty analysis. However, comparisons between the two approaches are presented, as well as experimental results.

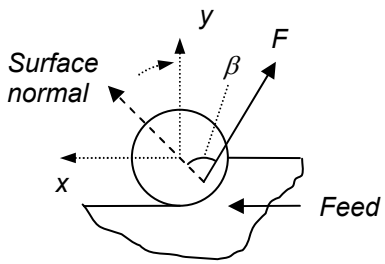

FIGURE 1. AVERAGE TOOTH POSITION APPROXIMATION FOR TLUSTY ANALYSIS.

STABILITY ANALYSES REVIEW

Although the Tlusty *et al*. and Altintas and Budak approaches are available in the literature, they will be summarized here to: 1) identify the input variables; and 2) make the paper self contained.

Tlusty *et al*. analysis

In this approach, an approximate analytical solution to the time-delayed differential equations of motion for milling is obtained by assuming an average position of the tooth in the cut (defined by the radial immersion). The cutting force, F, inclined at an angle β relative to the surface normal for this average position is projected into the x (feed) and y directions within the plane of the cut and then into the surface normal. In this way, the real part of the 'oriented' frequency response function, $G_{orient}(\omega) = \mu_x G_x + \mu_y G_y$, is determined, where ω is the circular frequency (rad/s), $\mu_{x/y}$ are the projections (or directional orientation factors) and $G_{x/y}$ are the real parts of the x and y direction frequency response functions (or FRFs) measured at the free end of the cutting tool, or tool tip (assuming the workpiece is rigid relative to the tool). Figure 1 depicts the average cutting tooth position for a 50% radial immersion down milling situation.

The limiting axial depth of cut, b_{lim}, is then defined as a function of G_{orient}, the cutting force coefficient, K_s, which relates F to the cross-sectional area of the uncut chip, and m^*, the average number of teeth engaged in the cut. See Eq. 1. Equation 2 relates the chatter frequency, ω_c (rad/s), should it occur, to spindle speed, Ω (rev/s), so that the stability lobe diagram may be plotted. In Eq. 2, m is the number of cutter teeth, N = 0, 1, 2, … is the integer number of vibration waves between teeth (lobe number), and ε (rad) is defined in Eq. 3, where H_{orient} is the imaginary part of the oriented FRF.

$$b_{lim} = \frac{-1}{2K_s G_{orient} m^*} \tag{1}$$

$$\frac{\frac{\omega_c}{2\pi}}{\Omega m} = N + \frac{\varepsilon}{2\pi} \tag{2}$$

$$\varepsilon = 2\pi - 2 \cdot \tan^{-1}\left(\frac{G_{orient}}{H_{orient}}\right) \tag{3}$$

Altintas and Budak analysis

In the Altintas and Budak approach, the time varying coefficients of the dynamic milling equations, which depend on the angular orientation of the cutter as it rotates through the cut, are expanded into a Fourier series and then truncated to include only the average component. The stability analysis is posed as an eigenvalue problem similar to the form det (A - λI) = 0, where λ represents the system complex eigenvalues and A is defined in Eq. 4, where $G_{x/y}$ and $H_{x/y}$ are again the real and imaginary parts of the tool point FRFs in the x and y directions, respectively. The terms α_{xx}, α_{xy}, α_{yx}, and α_{yy} depend on the selected radial immersion and the cutting force coefficient, K_r, which relates the radial cutting force component, F_r, to the tangential cutting force component, F_t, as shown in Eq. 5.

$$A = \begin{bmatrix} \alpha_{xx}(G_x + iH_x) & \alpha_{xy}(G_y + iH_y) \\ \alpha_{xy}(G_x + iH_x) & \alpha_{yy}(G_y + iH_y) \end{bmatrix} \tag{4}$$

$$F_r = K_r F_t \tag{5}$$

The resulting stability relationships are shown in Eqs. 6-8, where K_t relates F_t to the uncut chip area and the remaining variables are defined as before. The reader may note that these equations differ slightly from those in [Altintas and Budak] because the eigenvalue problem has been recast to match the format expected by Matlab™, the software used in this study. The explicit relationships between the Tlusty *et al*. and Altintas and Budak cutting force coefficients are provided in Eqs. 9 and 10.

$$b_{lim} = \frac{2\pi \cdot Re(\lambda)}{mK_t\left(Re(\lambda)^2 + Im(\lambda)^2\right)}\left(1 + \left(\frac{Im(\lambda)}{Re(\lambda)}\right)^2\right) \quad (6)$$

$$\Omega = \frac{\omega_c}{m}\frac{1}{(\gamma + 2\pi \cdot N)} \quad (7)$$

$$\gamma = \pi - 2 \cdot tan^{-1}\left(\frac{Im(\lambda)}{Re(\lambda)}\right) \quad (8)$$

$$K_s = \sqrt{1 + K_r^{\,2}} \quad (9)$$

$$tan\beta = \frac{1}{K_r} \quad (10)$$

In both approaches, a number of stability lobes are computed (i.e., N = 0, 1, 2, …) which, when taken together, define the stability limit. For our purposes it was necessary to determine the stability boundary as a single curve for the range of selected spindle speeds. This boundary was obtained by: 1) selecting a spindle speed within the range of interest; 2) determining the two points on each of the N stability lobes (if applicable) that bracketed the selected speed; 3) linearly interpolating to find the b_{lim} values; and 4) recording the minimum b_{lim} value from all N lobes.

UNCERTAINTY CONTRIBUTORS

From the previous section, the analysis inputs are: 1) the tool point FRF; 2) the cutting force coefficients; and 3) radial immersion. The variances in these inputs lead to b_{lim} uncertainty. Additional details regarding the first two are provided in the following subsections. Although spindle speed uncertainty could also be incorporated so that confidence intervals are included in both the vertical (b_{lim}) and horizontal (Ω) directions on the stability lobe diagram, Ω is typically known quite well and has not been treated here.

Tool point FRF

There are many sources which can influence the machine-spindle-holder-tool FRF as reflected at the tool point. These include the tool overhang length, diameter, flute geometry, and material properties; the tool-holder connection stiffness and damping; the holder geometry and material properties; the holder-spindle connection stiffness and damping; and spindle variations. The source of the spindle variations could include changes in dynamic stiffness with rotating speed and thermal fluctuations [e.g., Shin, Jorgenson and Shin, Schmitz *et al*., Cao and Altintas], although the non-rotating tool point FRF measurement is typically assumed to provide a reasonable approximation of the spindle response at speed. An important consideration in identifying the FRF uncertainty is that it is a frequency dependent, complex function [Hall].

Cutting force coefficients

Cutting force models may be: developed by transformation of orthogonal cutting parameters such as shear angle, shear stress, and friction coefficient to the geometry in question; obtained from previously tabulated data; or determined from mechanistic identification. Because the cutting coefficients are a function of both the workpiece material and cutting tool characteristics (as well as the cutting conditions in some cases), the mechanistic approach is often applied.

In this method, cutting tests are completed for a selected radial immersion and axial depth at a range of chip loads. The mean cutting forces for each chip load are recorded and a linear regression to the data is performed [Altintas]. The slope values for the x and y direction mean force data, m_x and m_y, are then used to determine the coefficients; Eqs. 11 and 12 give the expressions for slotting. One potential influence not often considered is variation in the coefficients with spindle speed.

$$K_t = \frac{4m_y}{Nb} \quad (11) \qquad K_r = \frac{-4m_x}{K_t Nb} \quad (12)$$

NUMERICAL STUDY

In this section a comparison of the spindle speed dependent uncertainty for the Tlusty and Altintas and Budak stability lobes is provided. Single degree of freedom, lumped parameter dynamics have been assumed in the x and y directions. The natural frequency, f_n, stiffness, k, and viscous damping ratio, ζ, values for the slightly asymmetric dynamics are listed in Table 1. A frequency dependent uncertainty equal to 15% of the magnitude at any given point on the real and imaginary curves was applied. The cutting force coefficients and standard deviations, σ, are provided in Table 2. Note that the K_t/K_r and K_s/β means and standard deviations are equivalent. The cutter was selected to have two teeth. Results for two radial immersions are presented: 1) 25% down milling (a radial depth of cut uncertainty of 25 μm was assumed); and 2) 100% radial immersion, or slotting (no radial depth uncertainty was applied).

TABLE 1. SYSTEM DYNAMICS MEAN VALUES FOR NUMERICAL CASE STUDY.

	f_n (Hz)	k (N/m)	ζ
x	1000	$8\text{x}10^6$	0.02
y	950	$7\text{x}10^6$	0.02

TABLE 2. CUTTING COEFFICIENTS AND STANDARD DEVIATIONS FOR NUMERICAL CASE STUDY.

	Mean	σ
K_s	794 N/mm^2	121 N/mm^2
β	71.8 deg	6 deg
K_t	750 N/mm^2	100 N/mm^2
K_r	0.33	0.06

Monte Carlo simulations were completed to determine the mean stability limit and $2u_c$, or 95%, confidence intervals (1000 repetitions). In these simulations, it was necessary to define the correlation between input variables. We assumed 100% correlation between individual frequencies, real and imaginary parts, and the x and y directions for the frequency response functions. This is based on the observation that physical changes to the tool-holder-spindle system can impact both the x and y directions at approximately the same level. We also assumed 100% correlation between the K_t/K_r and K_s/β pairs because they are computed from cutting forces obtained in a single test (when using the mechanistic approach). All other correlations were taken to be zero. Normal distributions were assumed in all cases.

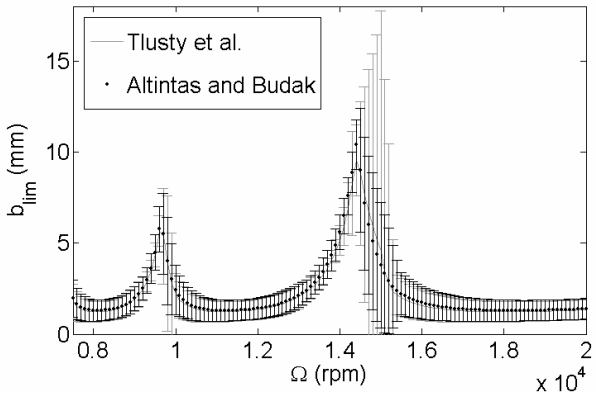

FIGURE 2. NUMERICAL RESULTS FOR 25% RADIAL IMMERSION.

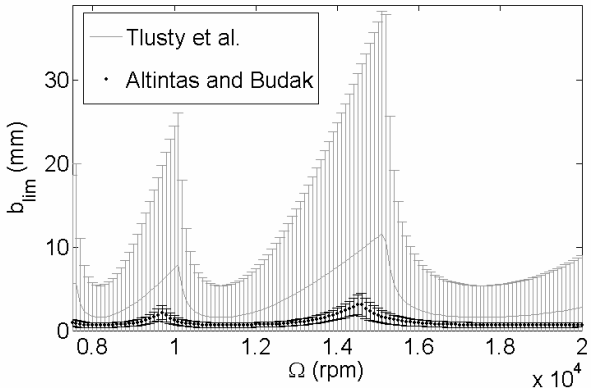

FIGURE 3. NUMERICAL RESULTS FOR 100% RADIAL IMMERSION.

Results for the 25% radial immersion case are shown in Fig. 2. The mean stability boundaries agree, while the uncertainty for the Tlusty approach (gray lines) gives increased uncertainty to the right of the stability lobe peaks. Slotting results are shown in Fig. 3. Here the mean predictions diverge substantially (also reported in [Altintas and Weck]). This is due to the average cutting tooth orientation assumed in the Tlusty *et al*. approach. Because the associated surface normal in slotting is parallel to the x direction, the y dynamics have no influence on the stability boundary (i.e., the projection is zero). The uncertainty for the Tlusty *et al*. lobes is also much larger. This is again a function of the average cutting direction. Because the x direction projection is (cos β) in slotting, this case is highly sensitive to β variations. Figure 4 demonstrates this high

sensitivity by comparing the results from using the mean value of β from Table 2 with zero standard deviation to the mean value with the standard deviation (from Table 2). As expected, the mean stability limits agree, but the uncertainty is significantly reduced when no variation in β is allowed.

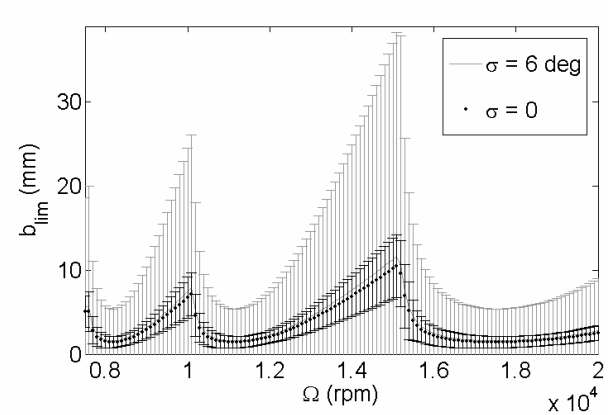

FIGURE 4. COMPARISON OF TLUSTY ET AL. LOBES FOR SLOTTING WITH AND WITHOUT VARIATION IN β.

EXPERIMENTAL RESULTS

Input data uncertainty evaluations

As noted previously, the primary uncertainty contributors in the stability limit calculations are the tool point FRF and the cutting force coefficients. In the following sections, we provide experimental results and uncertainty identifications for a particular setup.

Tool point FRF. A 12.7 mm diameter, 4 flute, 30 deg helix solid carbide end mill was inserted in a shrink fit holder with an overhang length of 70 mm and clamped in a 20000 rpm spindle. The non-rotating tool point frequency response was recorded in the *x* and *y* directions five times using impact testing. Between each test, the holder-tool was removed from the spindle and replaced. Further, the spindle was run at speeds of {5000, 10000, 15000, and 20000) rpm for 30 seconds between the tests to include potential thermal effects. The five measurements and 95% confidence intervals about the mean value for the *x* and *y* directions are shown in Figs. 5 and 6. The increased variation in the *y* direction results at the maximum amplitude is caused by an interaction between a spindle mode and the tool fundamental bending mode near 2000 Hz [Duncan *et al.*].

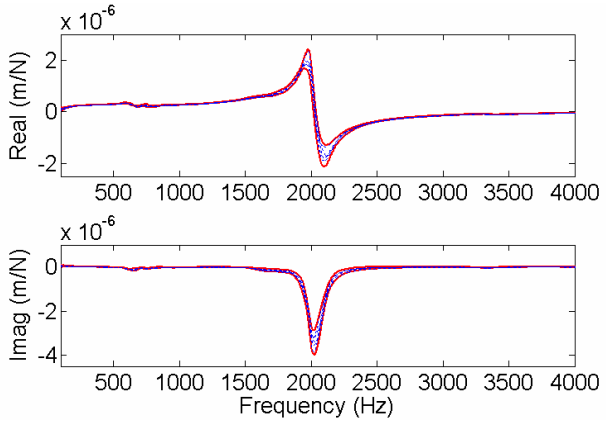

FIGURE 5. X DIRECTION FRF. MEASUREMENTS ARE SHOWN AS DOTTED LINES; 95% CONFIDENCE INTERVALS AS SOLID LINES.

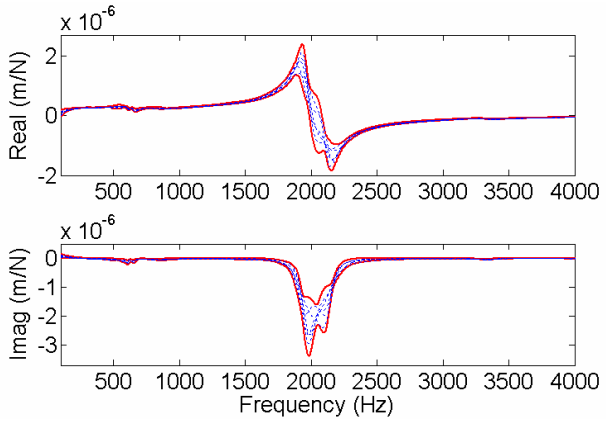

FIGURE 6. Y DIRECTION FRF. MEASUREMENTS ARE SHOWN AS DOTTED LINES; 95% CONFIDENCE INTERVALS AS SOLID LINES.

TABLE 3. CUTTING COEFFICIENT DATA FOR 7475 ALUMINUM.

Ω (rpm)	K_t (N/mm^2)			K_r		
1000	817	815	863	0.289	0.301	0.351
8900	670	702	686	0.213	0.208	0.157
Mean	759			0.253		
σ	82.2			0.072		

Cutting force coefficients. Slotting tests were performed in 7475 aluminum to mechanistically identify the cutting force coefficients. Tests were performed at two different spindle speeds, 1000 rpm and 8900 rpm, with each set repeated three times (six total data sets). Further, the 1000 rpm cuts were completed with an axial depth of 3.05 mm and

the 8900 rpm cuts with an axial depth of 1.02 mm. The chip loads for both cases were {0.03, 0.05, 0.10, and 0.15} mm/tooth. The variable cutting conditions were included to incorporate their potential influence on the cutting coefficients and the resulting variance in the mean values. Using the linear regression analysis described previously, K_t and K_r values were determined for all six data sets. See Table 3, where the mean values and standard deviations are also provided. The correlation between K_t and K_r was determined to be 97%. This relationship exists because the *x* and *y* cutting force data used to compute the coefficients are collected simultaneously during each cutting test (at the different chip loads) and exhibit ~100% correlation. The equivalent values for the Tlusty *et al*. coefficients were calculated using the relationships shown in Eqs. 9 and 10.

Stability lobe verification

The Monte Carlo simulation procedure requires selecting random samples from the input variable distributions and computing the output over many iterations. As noted, in this study it was necessary to consider the correlation between input variables.

For the FRF data, we applied 100% correlation between individual frequencies and between the real and imaginary parts of the complex response. In other words, a single random value (from a unit variance normal distribution) was used to select the real and imaginary values at each frequency of the FRF. See Eq. 13, where *a* is the random variable, *F* is the input variable value for a given iteration of the Monte Carlo simulation, $\bar{F}$ is its mean value, and σ_F is the standard deviation. The strong correlation between frequencies and real/imaginary parts occurs because the data is collected simultaneously in impact testing. It should be noted, however, that the uncertainty was frequency dependent, i.e., σ_F was a function of frequency in Eq. 13, and was larger near resonance as shown in Figs. 5 and 6.

$$F = \bar{F} + a \cdot \sigma_F \tag{13}$$

Another consideration for the FRF data was potential correlation between the *x* and *y* direction measurements. It is possible that if the variation between measurements was caused by, for example, a change in the connection between the holder and spindle, then both directions could be influenced in a similar manner. Therefore, we evaluated the covariance between the FRFs measured in the two directions, σ_{xy}. The result is shown in Fig. 7; it is seen that the covariance is strongly dependent on frequency with the highest values near resonance and near zero levels everywhere else. Because we already identified 100% correlation between frequencies and the real and imaginary parts for the individual directions, it was not possible to allow a frequency dependent correlation between the two directions. Therefore, we elected to observe zero correlation (between the *x* and *y* directions) as the generally more conservative approach[1].

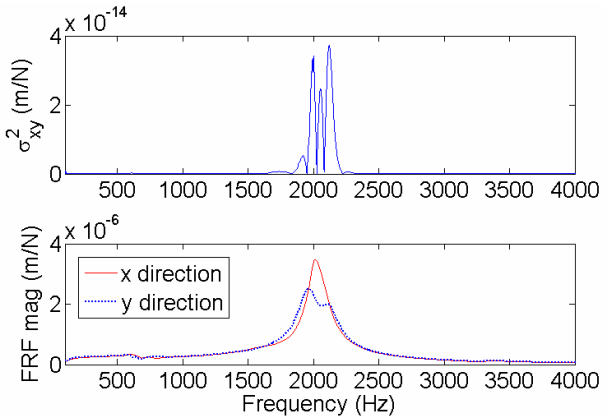

FIGURE 7. (TOP PANEL) COVARIANCE BETWEEN X AND Y DIRECTION FRFS. (BOTTOM PANEL) X AND Y DIRECTION FRF MAGNITUDES.

For the cutting force coefficients, 100% correlation was applied (i.e., the same random variable was used to sample both K_t and K_r, or, equivalently, K_s and β). The mean values and standard deviations provided in Table 3 were used.

Results for 25% radial immersion down milling tests at a range of spindle speeds between 10000 rpm and 20000 rpm (in increments of 1000 rpm) are shown in Figs. 8 and 9. At each speed, the axial depth was incrementally increased until chatter was observed. Unstable cuts were identified using the spectrum of the sound signal recorded during the cut [Delio *et al*.], as well as by the

[1] For completeness, Monte Carlo simulations were executed for the limiting cases of zero and 100% correlation. The results were practically identical.

nature of the machined surface finish. Figure 8 shows a comparison between the Altintas and Budak lobes with $2u_c$ confidence intervals and the cutting tests results, while Fig. 9 shows the Tlusty *et al.* lobes and experimental data. [Note the different vertical scales.] For the Monte Carlo simulations, 1000 iterations were completed and a radial depth of cut uncertainty of 25 μm was assumed.

A comparison of the two plots shows that the confidence intervals for the Tlusty *et al*. lobes are wider for equivalent input mean values, distributions, and correlations. In addition, the Tlusty *et al*. mean stability boundary tends to over predict the experimental stability limit for these tests. This may be the result of the asymmetric *x* and *y* direction FRFs.

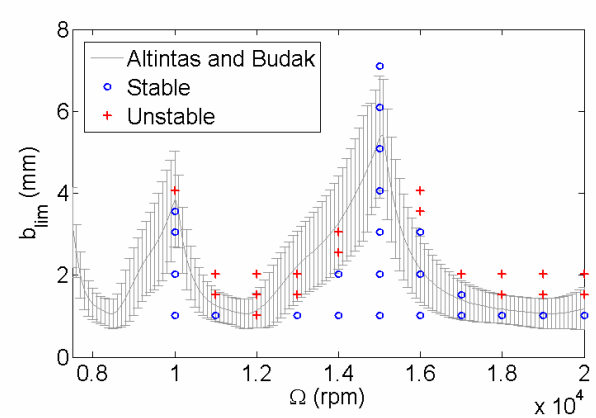

FIGURE 8. COMPARISON BETWEEN ALTINTAS AND BUDAK LOBES AND EXPERIMENTAL RESULTS. THE MEAN STABILITY BOUNDARY AND $2u_c$ INTERVALS ARE SHOWN.

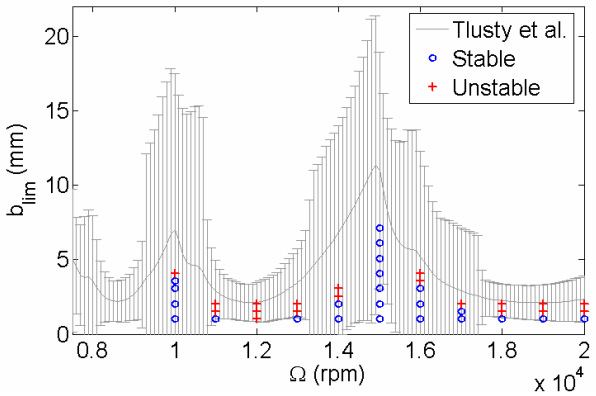

FIGURE 9. COMPARISON BETWEEN TLUSTY *ET AL*. LOBES AND EXPERIMENTAL RESULTS. THE MEAN STABILITY BOUNDARY AND $2u_c$ INTERVALS ARE SHOWN.

To interpret the confidence intervals in both cases, this region represents the axial depths, at the corresponding spindle speeds, where the cuts can either be stable or unstable (the shape of the distribution varies with the stability behavior and, therefore, spindle speed). Above the upper bound, cuts are expected to be unstable, while cuts should be stable below the lower bound (with 95% confidence). It is seen that these trends hold for the Fig. 8 data, except at 15000 rpm where a stable cut was recorded above the confidence interval. The wider intervals in Fig. 9 encompass all the unstable and the majority of the stable cuts.

CONCLUSIONS

This paper described a procedure for adding uncertainty bounds to the analytical milling stability limits predicted by the Tlusty *et al*. and Altintas and Budak approaches. This is an important consideration if users of the data are to evaluate their confidence in the predicted results, which is necessary for rational decision making. The primary uncertainty contributors included the tool point frequency response functions and the cutting force coefficients, which relate the cutting force to the uncut chip area. Monte Carlo simulation was used to propagate the input uncertainties through the analytical equations and determine the mean stability limit and associated spindle speed dependent uncertainties. For the cutting tests completed as part of this work, the Altintas and Budak results demonstrated closer agreement with experiment. However, the procedure should be applied to additional tests to verify the performance (and uncertainty) of both methods over a broader range of cutting conditions.

ACKNOWLEDGEMENTS

This work was partially supported by the National Science Foundation (DMI-0238019), Office of Naval Research (Young Investigator Program), and TechSolve. Any opinions, findings, and conclusions or recommendations expressed in this material are those of the authors and do not necessarily reflect the views of these organizations. The authors would also like to acknowledge helpful discussions with Dr. R. Haftka, University of Florida.

REFERENCES

Altintas, Y., (2000), Manufacturing Automation, Cambridge University Press, Cambridge, UK.

Altintas, Y. and E. Budak, (1995), "Analytical Prediction of Stability Lobes in Milling", *Annals of the CIRP*, Vol. 44/1, pp. 357-362.

Altintas, Y. and M. Weck, (2004), "Chatter Stability of Metal Cutting and Grinding", *Annals of the CIRP*, Vol. 53/2, pp. 629-642.

American National Standards Institute, (1997), ANSI/NCSL Z540-2-1997, *US Guide to the Expression of Uncertainty in Measurement*.

Bevington, P.R. and D.K. Robinson, (1992), *Data Reduction and Error Analysis for the Physical Sciences*, 2nd Edition, WCB/McGraw-Hill, Boston, MA.

Cao, Y. and Y. Altintas, (2004), "A General Method for the Modeling of Spindle-Bearing Systems", *ASME Journal of Mechanical Design*, Vol. 126, pp. 1089-1104.

Delio, T., J. Tlusty, J., and K.S. Smith, (1992), "Use of Audio Signals for Chatter Detection and Control", *Journal of Engineering for Industry*, Transactions of the ASME, Vol. 114, pp. 146-157.

Duncan, G.S., M. Tummond, and T. Schmitz, (2005), "An Investigation of the Dynamic Absorber Effect in High-Speed Machining," *International Journal of Machine Tools and Manufacture*, Vol. 45, pp. 497-507.

International Standards Organization (ISO), (1993), *Guide to the Expression of Uncertainty in Measurement* (Corrected and Reprinted 1995).

Jorgenson, B., and Y. Shin, (1998), "Dynamics of Spindle-Bearing Systems at High Speeds Including Cutting Load Effects", *ASME J. of Manufacturing Science and Engineering,* Vol. 120, pp. 387-394.

Schmitz, T.L., J. Ziegert, and C. Stanislaus, (2004), "A Method for Predicting Chatter Stability for Systems with Speed-Dependent Spindle Dynamics", *Transactions of NAMRI/SME*, Vol. 32, pp. 17-24.

Shin, Y., (1992), "Bearing Nonlinearity and Stability Analysis in High-Speed Machining", *ASME J. of Engineering for Industry*, Vol. 114, pp. 23-30.

Taylor, B.N. and C.E. Kuyatt, (1994), "Guidelines for Evaluating and Expressing the Uncertainty of NIST Measurement Results", *NIST Technical Note 1297 1994 Edition*.

Tlusty, J., W. Zaton, W., and F. Ismail, (1983), "Stability Lobes in Milling", *Annals of the CIRP*, Vol. 32/1, pp. 309-313.